

Self-sealing experiments and gas injection tests in a backfilled microtunnel of the Mont Terri URL

G. W. LANYON^{1*}, P. MARSCHALL², T. TRICK³, R. DE LA VAISSIÈRE⁴,
H. SHAO⁵ & H. LEUNG⁶

¹*Fracture Systems Ltd, St Ives, Cornwall, UK*

²*National Cooperative for the Disposal of Radioactive Waste,
5430 Wettingen, Switzerland*

³*Solexperts AG, 8617 Mönchaltorf, Switzerland*

⁴*French National Agency for Radioactive Waste Management, 55290 Bure, France*

⁵*Federal Institute for Geosciences and Natural Resources, 30655 Hannover, Germany*

⁶*Nuclear Waste Management Organization, Toronto, Ontario, Canada*

*Corresponding author (e-mail: bill@fracture-systems.co.uk)

Abstract: This paper describes a large-scale experiment on gas transport and hydromechanical processes around underground structures as part of a long-term geoscientific research programme at the Mont Terri Underground Rock Laboratory in the Jura Mountains of Switzerland. A horizontal microtunnel with a diameter of 1 m and a length of 13 m was drilled in an over-consolidated claystone formation. After installing monitoring instruments in the open tunnel, the end of the tunnel was backfilled with sand (test section) and a large hydraulic packer was emplaced in the seal section. The packer was inflated and subsequently the test interval was saturated with a synthetic pore-water. Following saturation an extended programme of hydraulic testing was performed over a two year period. A series of gas injection tests was then performed over a period of approximately 1.5 years. Following this first series of gas injections, a long post-gas hydraulic test has been initiated. The paper presents data and interpretation of the gas injections and subsequent hydraulic testing. The ability of the excavation damage zone to transport gas at pressures below fracturing is demonstrated. The post-gas hydraulic performance is considered and related to the self-sealing of the damage zone observed during saturation and hydraulic testing.

The investigation of damage zones around excavations such as seal sections in tunnels or shafts and their impact on gas migration are key issues in the field of underground waste disposal. The experiment ('Gas path through host rock and along seal sections/HG-A') was designed as a long-term gas experiment in a backfilled microtunnel, to investigate both leak-off rates and gas release paths from a sealed tunnel section in an ultra-low permeability host rock (Opalinus Clay). The aims of the HG-A experiment are to:

- provide evidence for barrier function of the Opalinus Clay on the tunnel scale (scale effects in rock permeability);
- investigate self-sealing of the excavation damage zone (EDZ) after tunnel closure (mechanical self-sealing in response to packer inflation and pore pressure changes);
- provide evidence for gas transport capacity of Opalinus Clay (intact host rock and EDZ).

The Opalinus Clay

The Opalinus Clay in Northern Switzerland has been identified as a potential host rock formation for the disposal of radioactive waste (Nagra 2002). The formation is part of a thick Mesozoic–Cenozoic sedimentary sequence which was deposited 180 Ma ago in a shallow marine environment.

At Mont Terri the Opalinus Clay formation reached a maximum depth of about 1000 m and can be classified as a slightly overconsolidated rock, the estimated overconsolidation ratio varying between 2.5 and 3.5 (estimates derived from both laboratory tests and burial history). The principal stress σ_1 at laboratory level is in the order of 6.5 MPa, subvertically oriented, and it reflects the overburden; σ_3 is NE–SW-oriented (2.5 MPa) and σ_2 runs in a NW–SE direction (4.5 MPa) parallel to the Security Gallery (Fig. 1; Martin *et al.* 2002). There is some uncertainty on the stress tensor, in particular relating to the magnitude of

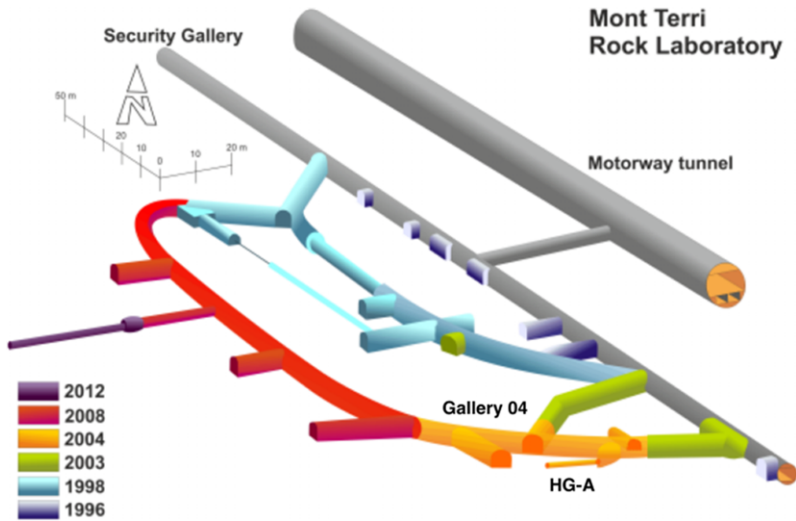


Fig. 1. Layout of the Mt Terri Rock URL. Tunnels are coloured by year of excavation. The HG-A experiment niche and microtunnel are visible at the bottom right of the figure.

σ_3 (see Martin & Lanyon 2003 and Corkum & Martin 2007).

Quantitative laboratory analyses of core samples from Mont Terri showed a total mass fraction of clay minerals of 47–60%, a quartz content of 14–30% and 16–22% carbonates. The fraction of swelling clay minerals of 23–27% (illite, illite/smectite mixed layers) is of particular relevance for the consolidation behaviour of the rock. Further minerals are siderite, pyrite and feldspar (Pearson *et al.* 2003).

Intact Opalinus Clay at Mont Terri exhibits a very low hydraulic conductivity, with a mean hydraulic conductivity of $2 \times 10^{-13} \text{ m s}^{-1}$, and a moderate spatial variability, which is less than an order of magnitude (Marschall *et al.* 2004). Microscopic observation of the fabric of the Opalinus Clay at Mont Terri suggests that there may be a significant core-scale hydraulic anisotropy. The ratio between bedding-parallel and bedding-normal permeability is thought to lie between 1 and 10. The very fine pore network is saturated with a Na–Cl–SO₄ connate pore-water of marine origin with a mean content of dissolved solids of about 12 g l^{-1} . Even though the rock is fractured, a distinct fracture transmissivity has not been observed, suggesting that the fractures are generally tight for the given stress conditions.

Rock mechanical characterization of the Opalinus Clay is challenging owing to its ultra-low permeability, over-consolidation and distinct bedding. Typical values for key geotechnical parameters are shown in Table 1 (Bock 2000).

EDZ experiments at Mont Terri

Since its inception, EDZ experiments have been a focus of the Mont Terri programme (Thury & Bossart 1999; Bossart *et al.* 2004; Blümling *et al.* 2007). Experience from the experiments suggests that the damage zone geometry and properties are a function of:

- excavation method (drill and blast or mechanical methods);
- orientation of the tunnel relative to the *in situ* stress field and to the bedding fabric of the rock;
- excavation geometry (size and shape);
- presence of pre-existing faults and fractures;
- environmental conditions within the excavation (ventilation/humidity).

The HG-A experiment supplements results from previous EDZ experiments in terms of scale *c.* 1 m (intermediate between boreholes and tunnels) and orientation (bedding-parallel).

The response to excavation of the microtunnel and the associated creation and development of the EDZ is discussed in Marschall *et al.* (2006, 2008). The EDZ around the microtunnel is formed by the interaction of the rock and stress anisotropy with significant breakout zones ('notches') at 3 o'clock and 9–11 o'clock (see Fig. 10a).

The test section saturation and hydraulic testing prior to gas injection are presented in Lanyon *et al.* (2009). This paper presents the results of gas leak-off testing and subsequent post-gas hydraulic

SELF-SEALING AND GAS INJECTION TESTS

Table 1. *Geotechnical reference parameters of the Opalinus Clay at the Mont Terri Underground Laboratory (after Bock 2000)*

Parameter	Value	Remarks
Bulk density (mg m^{-3})	2.45	Water saturated
Grain density (mg m^{-3})	2.71	
Porosity (%)	13.7	Range: 10–16%
Water content (% wt)	6.1	Range: 6–7%
Young's modulus (GPa)	104	Parallel to bedding
Shear modulus	1.2	Normal to bedding
Poisson's ratio (–)	0.27	
Uniaxial compressive strength (MPa)	1016	Parallel to bedding
Tensile strength (MPa)	21	Normal to bedding
P-wave velocity (m s^{-1})	3410	Parallel to bedding
S-wave velocity (m s^{-1})	2620	Normal to bedding
Fracture toughness K_{IC} ($\text{MN m}^{-1.5}$)	1960	Parallel to bedding
	0.530	Normal to bedding

testing together with an overview of the rock's response to testing.

Experimental layout and sequence

The HG-A experiment is located in the southern part of the Mont Terri Rock Laboratory off Gallery 04 (see Fig. 1). The 1 m-diameter, 13 m-long microtunnel was excavated during February 2005 using a steel auger from a niche in Gallery 04. The microtunnel was excavated parallel to bedding strike and bedding parallel features run along the tunnel, replicating the expected relationship between bedding and emplacement tunnel orientation in a deep repository (Nagra 2002), where bedding is expected to be flat-lying and emplacement tunnels to be subhorizontal. The excavation was monitored by a borehole array containing piezometers and deformation gauges (clino-chain and chain deflectometers). The borehole array was subsequently augmented with additional piezometer boreholes and borehole stress meters (Fig. 2a).

The first 6 m of the microtunnel was lined with a steel casing immediately after excavation to stabilize the opening. The gap behind the liner was then cement-grouted, but not sealed. The purpose-built hydraulic megapacker (diameter 940 mm and sealing section length 3000 mm) was installed in 2006. The sealing section was located at 6–9 m with a 1 m grouted zone containing the non-sealing part of the packer and retaining wall from 9–10 m. The final 3 m of the microtunnel from 10–13 m forms the test section which was instrumented and backfilled prior to packer emplacement (see Fig. 2b).

Instrumentation

The test section was instrumented with piezometers, extensometers, strain-gauges and time domain

reflectometers (TDRs) to measure pressure, deformation and water content. After instrumentation the test section was backfilled with sand behind a retaining wall (Fig. 2b).

The seal section was instrumented with piezometers, total pressure cells and TDRs prior to the installation of the megapacker. Following the installation of the megapacker the volume between the retaining wall and the megapacker was filled with a cement grout. Table 2 lists the instruments in the geosphere, test and sealing sections.

Saturation and long-term hydraulic testing

Saturation of the test section and surrounding rock was started in November 2006 following emplacement of the megapacker (June 2006) and subsequent grouting of the section between the megapacker and test section (see Fig. 3). A variety of saturation tests was performed using a synthetic pore-water (Pearson *et al.* 2003) until January 2008, when a long-term multirate hydraulic test was initiated (see Lanyon *et al.* 2009). This test continued until February 2010 and involved a series of constant rate injection steps. During the test the applied injection rate was reduced from *c.* 10 to 0.1 ml min^{-1} (144 ml per day). The results from the hydraulic testing indicated progressive self-sealing (Lanyon *et al.* 2009; Bock *et al.* 2010).

During hydraulic testing the effective stress conditions in the seal zone were altered by changing the megapacker pressure. At low megapacker pressures (*c.* 2000 kPa) the minimum measured radial stress was *c.* 1600 kPa, which was close to the then test section pressure, resulting in very low effective stress conditions and apparently higher EDZ permeability (Lanyon *et al.* 2009). Since June 2009 the megapacker pressure has been maintained above 2600 kPa with measured total pressures in

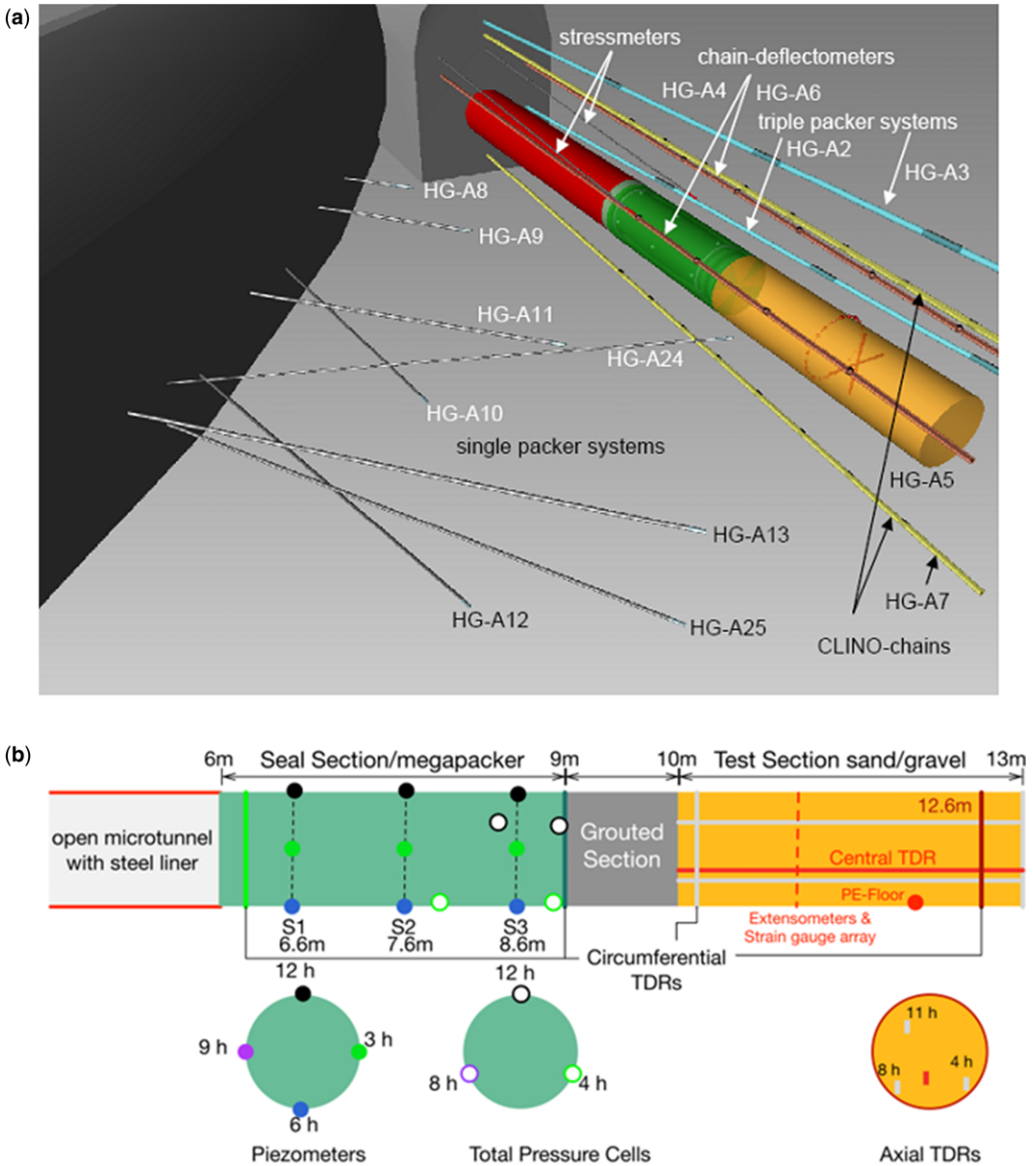


Fig. 2. Schematic drawing of the microtunnel and the site instrumentation: (a) layout and borehole instrumentation (colour coding refers to the steel liner, red; the seal section, green; and the backfilled test section, orange); (b) seal section and test section instrumentation.

the sealing section always above 1950 kPa, considerably above the test section pressure.

Immediately prior to the start of the gas injection phase the water injection was reduced from 0.1 to 0.04 ml min⁻¹ to lower the initial pressure in the test section. This resulted in a test section pressure prior to gas injection of 300 kPa absolute.

Gas injection phase

The gas injection phase included three separate nitrogen gas injections, listed in Table 3; microtunnel sensor responses to gas injection are shown in Figure 4. After each gas injection, following a shut-in period, water was extracted from the test section and depressurized to remove trapped gas

SELF-SEALING AND GAS INJECTION TESTS

Table 2. *HG-A experiment instrumentation*

Instrument	Count	Measurement
<i>Test section instrumentation</i>		
Piezometers	2	Pore pressure
Extensometers	2	Horizontal/vertical deformation
Strain gauges	22	Circumferential deformation
TDRs	8	Volumetric water content
Geophones	8	Acoustic emission
<i>Seal section instrumentation</i>		
Piezometers	12	Pore pressure
Total pressure cells	6	Load on tunnel wall + temperature
TDRs	2	Volumetric water content
<i>Geosphere instrumentation</i>		
Piezometers	14	Pore pressure
Deflectometers	2	Deformation (8-point)
Clino-chains	2	Deformation (8-point)
Stressmeters	3	Deformation and stress + temperature

(gas–water exchange). The degassed water was then re-injected into the test section. This procedure provided a well-defined initial gas saturation in the test section pore-water for the subsequent gas injection. During gas injection a low constant rate (c. 0.02 ml min^{-1}), water injection was maintained in the test section.

Pressure response to gas injection

Gas pressure during GI1 was limited to 1200 kPa, significantly below the minimum stress, to avoid coupled mechanical effects. After an initial 20 ml N min^{-1} injection when pressure rose quickly, the injection rate was reduced to about 10 ml N min^{-1}

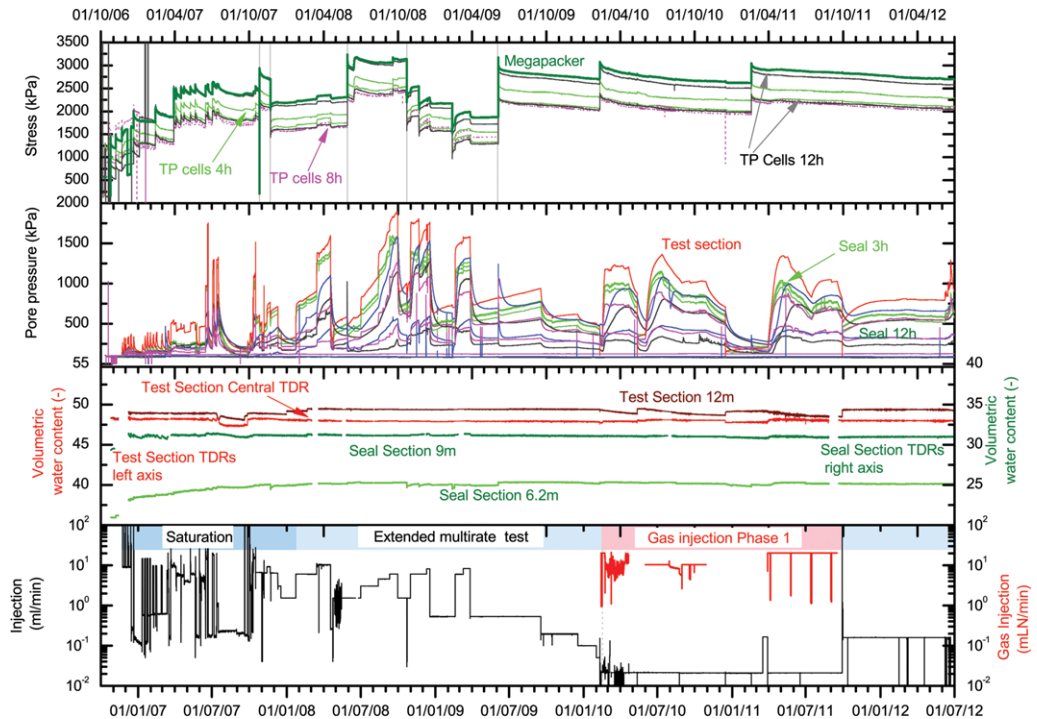
**Fig. 3.** Microtunnel stress, pore pressure, water content and flow rate measurements from start of saturation.

Table 3. Gas injection steps

	Injection Rate (ml N min ⁻¹)	Duration (days)	P_0 (kPa)	P_{max} (kPa)	Total gas volume (l N)
GI1	20 switching to constant pressure c. 1200 kPa	65	290.2	1234	1028
GI2	10.3	149	361.6	1363	2096
GI3	20.3	171	204.2	1347	4864

to maintain an approximately constant test section pressure.

During GI2 test section pressure rose more slowly than in GI1 and then peaked at 1363 kPa on 12 July 2010. After the pressure breakdown, the test section pressure dropped over about a month by about 350–975 kPa and then stabilized at about 1040 kPa.

During GI3, test section pressure again peaked at 1347 kPa but with a broader peak than in GI2 and then dropped to about 840 kPa owing to an interruption in injection before recovering (after resumption of gas injection) and stabilizing at about 1040 kPa.

Pressures in the sealing section during gas injection were lower and lagged those in the test section, as would be expected. Pressure response was highly heterogeneous, indicating a sparsely connected system of flow paths. Pressure along the 3 o'clock sensors reacted most strongly and quickly to the test section suggesting a high diffusivity connection. However, the pressure at section 1 (6.6 m) in PES-S1–3h (close to the rear of the sealing element) was high (in fact higher than PES-S2-3h a sensor in the centre of the seal section at 7.6 m) and comparable to PES-S3-3h (8.6 m) closest to the test section. This suggests that this piezometer is not well connected to the open tunnel. PES-S1-6h shows a small response but the other piezometers in section 1 show no response to gas injection and remain at close to atmospheric pressure.

After shut-in and depressurization, remnant high pressures were observed at some piezometers in the sealing section, indicating possible closure after gas injection or some other loss of connectivity, perhaps owing to water invasion and blocking.

Total pressure cells

The measured total pressures in the sealing section largely followed the applied megapacker pressure.

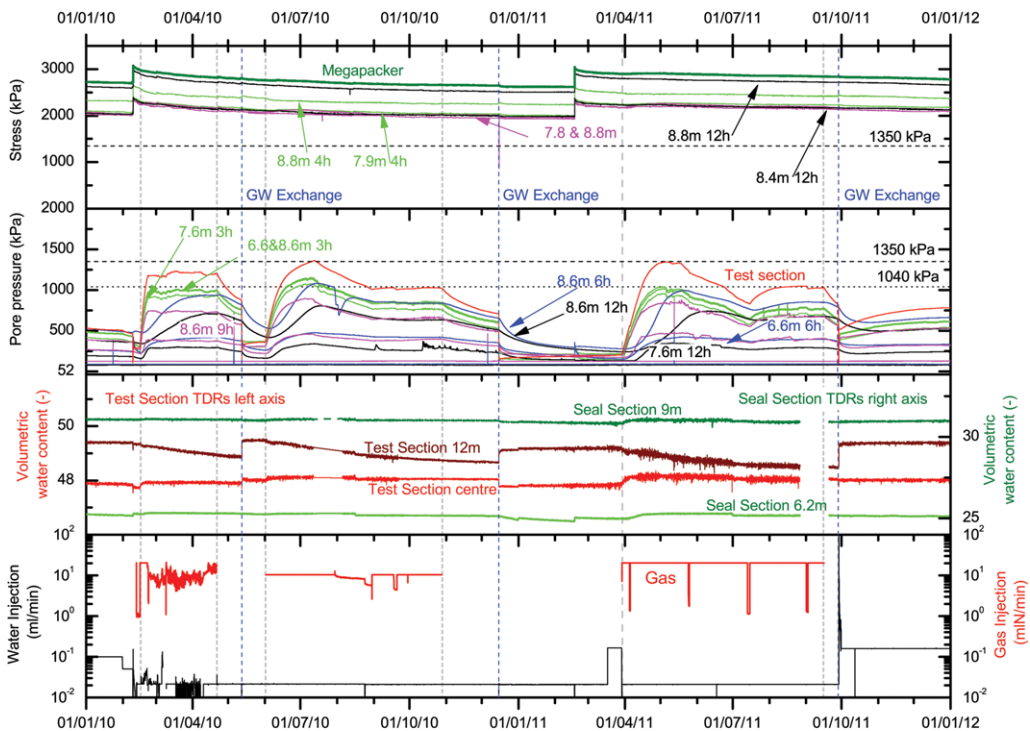


Fig. 4. Microtunnel stress, pore pressure, water content and flow rate measurements during gas injection. Gas–water exchange marked as vertical blue dashed lines. Sensor locations shown in Figure 2b.

SELF-SEALING AND GAS INJECTION TESTS

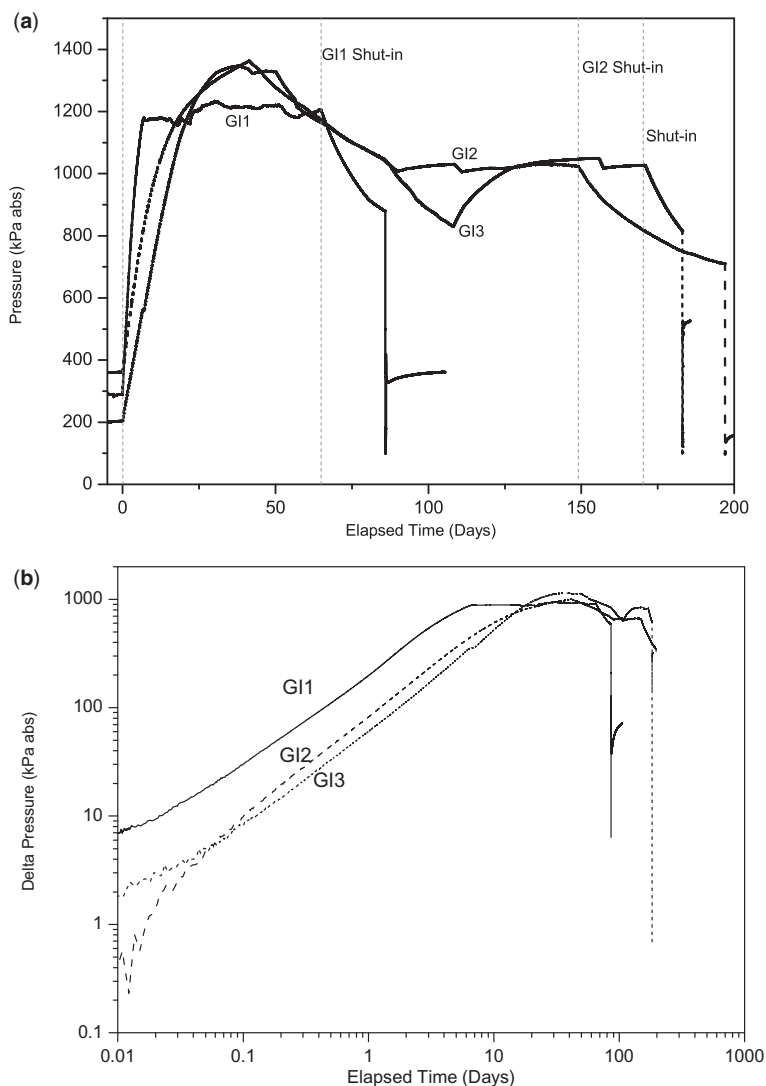


Fig. 5. (a) Linear and (b) log–log plots of delta pressure from GII–3.

Total pressures were typically 75–95% of the mega-packer pressure. Stresses were more heterogeneous in section 1 (7.85–8.36 m) than section 2 (8.84–8.87 m), although this could have been due to instrumentation offsets. The influence of test section pressure can be seen in the data, with load increasing slightly as test section pressure increases.

Temperature

Temperature was monitored within the laboratory, in the test section and geosphere throughout the experiment. The laboratory temperature showed a variable seasonal trend between 10 and 15 °C.

Borehole temperature data showed an attenuated seasonal response between 12 and 13 °C with a slight upward trend. Temperatures measured in the test section in a circumferential strain gauge array showed an overall slow increase similar to that measured in the geosphere. Two temperature gauges located at the top of the microtunnel showed irregular temperatures occurring after the start of each gas injection.

TDRs

The three circumferential TDRs showed a small reduction (*c.* 1%) in water content during gas

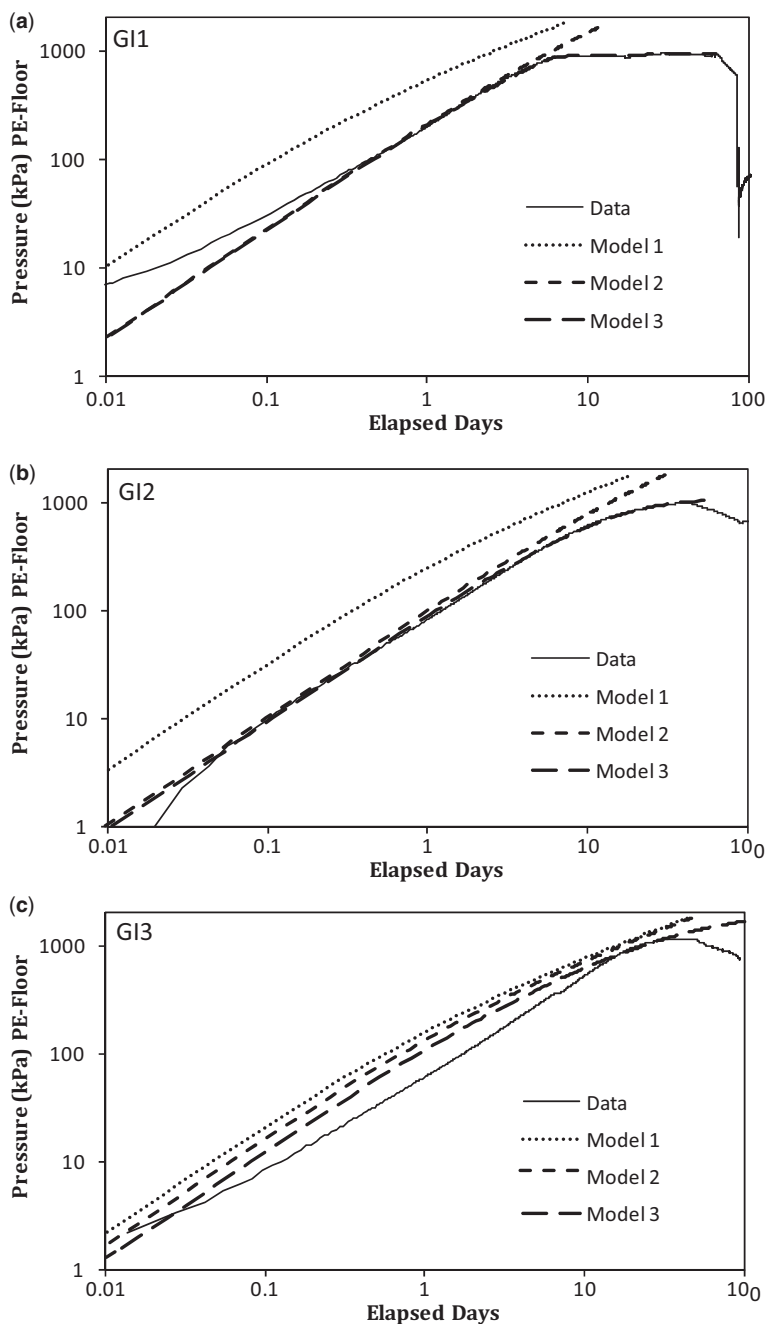


Fig. 6. Log-log plots of delta pressure (sensor PE-Floor) for each gas injection for models 1–3: (a) GI1; (b) GI2; (c) GI3.

injection which recovered after the gas–water exchange. The lack of recovery during shut-in and pressure drop and subsequent recovery after gas–water exchange suggest that this was a response to

the presence of gas rather than a coupled response owing to test section pressure. The responses were, however, small and would indicate that a totally desaturated zone might have existed over a small

SELF-SEALING AND GAS INJECTION TESTS

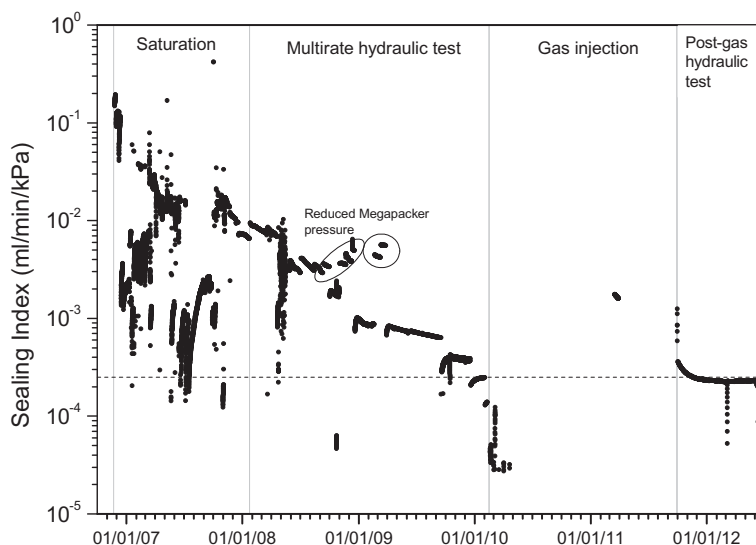


Fig. 7. Sealing index S during water injection. Periods of reduced megapacker pressure (resulting in low effective stress) are marked.

part of the circumference owing to a gas layer in the top of the test section. If the desaturation was only partial, the desaturated layer could have been thicker. The onset of response was slightly delayed from the start of gas injection, indicating possible dissolution or trapping of the first gas injected and the delay was greatest during GI2. The TDR at the rear of the test section showed a more delayed response as it did not extend to the top of the microtunnel.

The axial TDRs showed a different pattern with increased water content after the first gas–water exchange and small reductions midway through GI2. Water content dropped after the gas–water exchange and then increased at the start of GI3. This behaviour is difficult to explain and requires further consideration. It is possible that it reflects both changes in porosity within the sand/gravel as well as saturation. Alternatively it may have been an instrumentation artefact.

The sealing section TDRs showed significantly lower water content than the test section (contrast between porosity of rock and backfill) together with a minor reduction in water content after the GI2 gas–water exchange in both the 9.0 and 6.2 m section TDRs. This drop in water content recovered at the start of GI3. Again it is difficult to interpret these small responses.

Geosphere response

Pore pressure and strain responses (clinometer, deflectometer and borehole stress gauge) in the

geosphere showed responses largely related to the test section pressure similar to those observed during long hydraulic testing. No clear evidence of gas transport was obvious from the geosphere data.

Post-gas hydraulic testing

Following the final gas–water exchange, a constant rate 0.17 ml min^{-1} water injection into the test section was initiated to determine any effect of the gas testing on the water leak-off characteristics of the EDZ (via the sealing index). The test started on 30 September 2011 and is ongoing (September 2012).

Analysis

The HG-A experiment is being modelled by several groups both within the HG-A experiment and as part of the EU FORGE project (FORGE 2009). Numerical models including two-phase flow and hydromechanical coupling are being used to assess the complete experimental sequence. Here simple models are presented to consider pre-breakdown behaviour of the test section and self-sealing.

Pre-breakdown behaviour

Here we present an analytical model of the pre-breakdown response of the test section pressure illustrating the different processes. Figure 5 shows a comparison between the test section pressures in

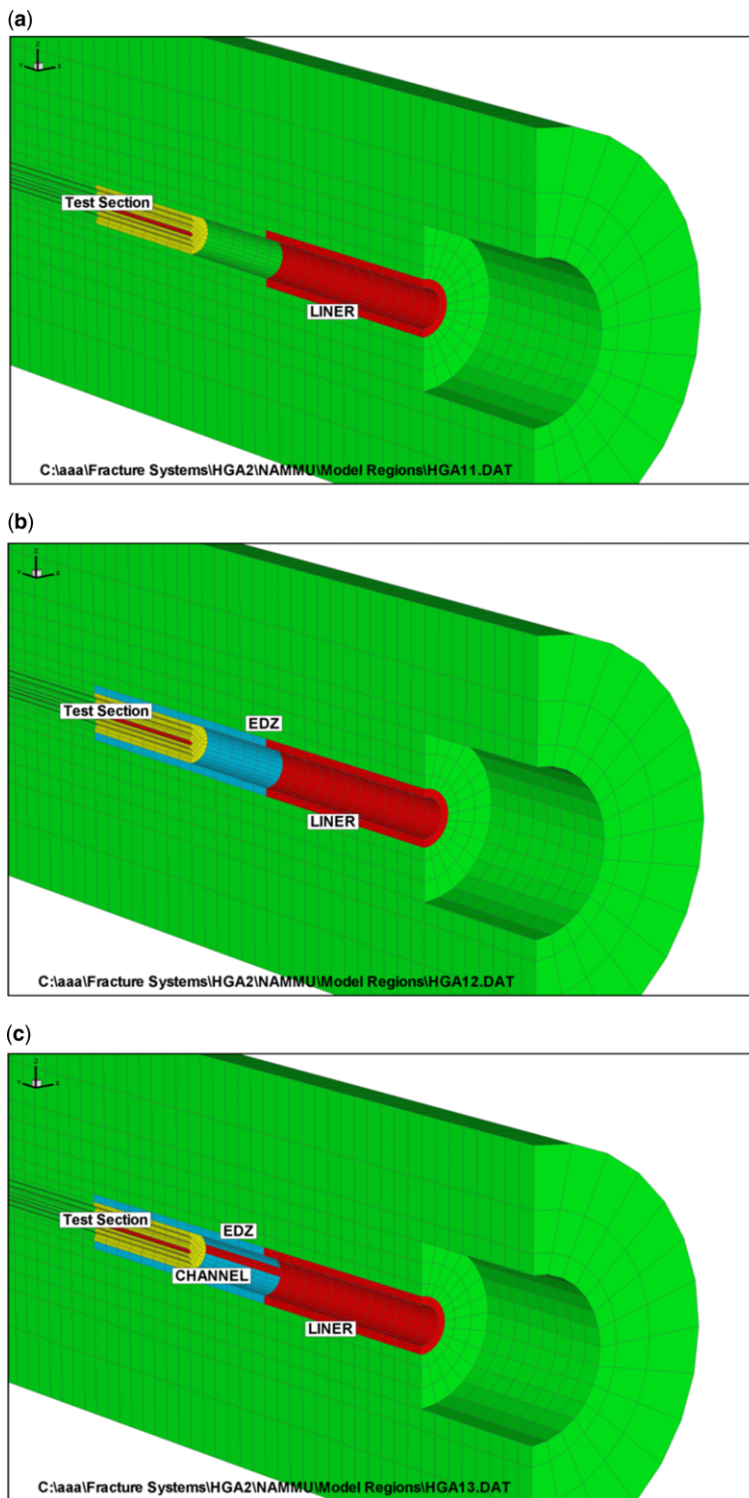


Fig. 8. Continuum models A, B and C from Lanyon *et al.* (2009).

SELF-SEALING AND GAS INJECTION TESTS

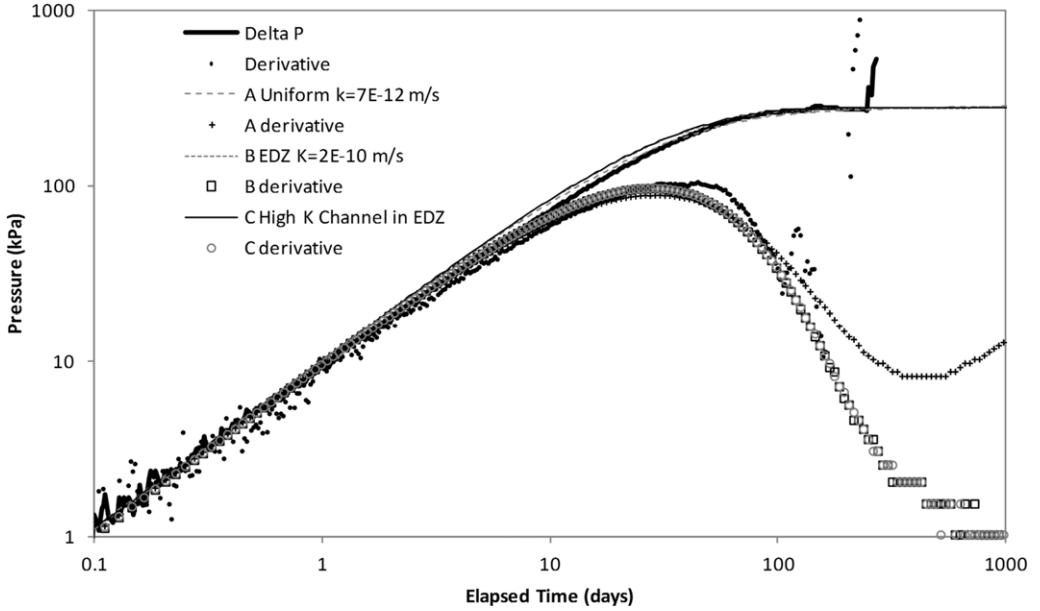


Fig. 9. Diagnostic plot from post-gas hydraulic test. Measured and calculated delta pressure and derivative.

GI1, GI2 and GI3. Inspection of the log–log plots (Fig. 5b) shows an approximately linear behaviour for the first 20 days prior to the subsequent breakdown in GI2 and GI3. In GI1 pressure is held constant and no breakdown was observed.

Predicted test section delta-pressures for GI1–3 from three simple models are shown in Figure 6a–c. The models describe the relationship between test section pressure P (kPa) and gas volume V (m^3).

Model 1: test section and gas compressibility only

$$\Delta P = C \cdot \Delta V; \quad \Delta V = q \Delta t$$

Model 2: compressibility and dilution

$$\Delta V = \left(q \Delta t - \frac{HM_w \Delta P}{P_0 \rho_{g0}} \right) \frac{P_0}{P}$$

Table 4. Rock hydraulic conductivity (m s^{-1}) fitted to post-gas hydraulic test for models A–C: (see Fig. 8)

Model	Rock	EDZ	Channel
A – no EDZ	7×10^{-12}		
B – cylindrical EDZ	10^{-13}	2×10^{-10}	
C – EDZ + channel	10^{-13}	10^{-11}	6×10^{-9}

Model 3: compressibility, dilution and leakage

$$\Delta V = \left(q \Delta t - \frac{HM_w \Delta P}{P_0 \rho_{g0}} \right) \frac{P_0}{P} - q_w \Delta t$$

The models are characterized by:

- q , gas injection rate (ml min^{-1} @ standard temperature and pressure);
- C , test section compressibility ($\text{m}^3 \text{kPa}^{-1}$);
- M_w , mass of water in test section (kg);
- q_w (ml min^{-1}) water leakage calculated from S , sealing index ($\text{ml min}^{-1} \text{kPa}^{-1}$).

Standard values for nitrogen properties (density ρ , Henry's law constant H) were used. Analysis of the long-term multirate test suggested a C of $10^{-5} \text{m}^3 \text{kPa}^{-1}$ and S of $5 \times 10^{-4} \text{ml min}^{-1} \text{kPa}^{-1}$ (see Fig. 7). M_w was estimated as 700 kg from the tunnel volume and an estimated porosity of 30%. These values together with the applied gas flow rate were used in models for GI1 and GI2, while for GI3 it was necessary to significantly increase the compressibility, possibly indicating that there was a significant amount of free gas in the test section prior to the start of GI3, despite the gas–water exchange.

Model 3, incorporating test section compressibility, gas dissolution and water leakage using parameters derived from the long term multirate test, is able to reproduce the pre-peak behaviour of

GI1 and GI2 (see Fig. 6a, b). The model is not able to replicate the response in GI3, suggesting that conditions had changed prior to GI3, probably owing to the presence of free gas. It is possible that leakage from the test section may also have changed after GI2, but such a change would be difficult to determine given uncertainty in initial conditions.

Self-sealing

Self-sealing of fractures in claystone rocks has been observed at Mont Terri and other sites (Bock *et al.* 2010). Lanyon *et al.* (2009) define a simple measure of the flow resistance across the seal section as the sealing index, S ($\text{ml min}^{-1} \text{kPa}^{-1}$) based on the injection rate and test section pressure as:

$$S = \frac{Q}{P_{\text{TestSection}} - 100 \text{ kPa}}$$

where Q is the flow into the test section in ml min^{-1} and $P_{\text{TestSection}}$ is the test section pressure in kPa absolute. This measure was chosen as it is not possible to determine equivalent permeability or hydraulic conductivity without assumptions concerning the geometry of the flow paths in the EDZ. Assuming linear flow and a flow-path length of 3 m (seal section), the sealing index can be converted into an EDZ conductance ($\text{m}^3 \text{s}^{-1}$) by multiplying by a factor 5×10^{-7} (considering only resistance along the seal section). Figure 7 shows the calculated sealing index after filtering data for flow rate changes affected by storage.

In the year prior to gas injection, the sealing index S reduced from 10^{-3} to almost 10^{-4} ($\text{ml min}^{-1} \text{kPa}^{-1}$), equivalent to a hydraulic conductance of $1-10 \times 10^{-11} \text{m}^3 \text{s}^{-1}$. After gas injection during the post-gas hydraulic testing, S quickly reduced to about $2.5 \times 10^{-4} \text{ml min}^{-1} \text{kPa}^{-1}$, only slightly higher than that prior to gas injection after a relatively short recovery.

A simple groundwater flow continuum model as described in Lanyon *et al.* (2009) has been used to model the post-gas hydraulic test for three different cases (see Fig. 8):

- (1) uniformly permeable rock, no EDZ;
- (2) cylindrical EDZ (40 cm thick) in uniform permeability rock;
- (3) channel in EDZ in uniformly permeable rock.

The hydraulic conductivity of the different rock types has been adjusted to provide a match to the observed delta-pressure as shown in Figure 9 and Table 4. It can be seen that the models with an EDZ (creating a 'linear' flow geometry) are a

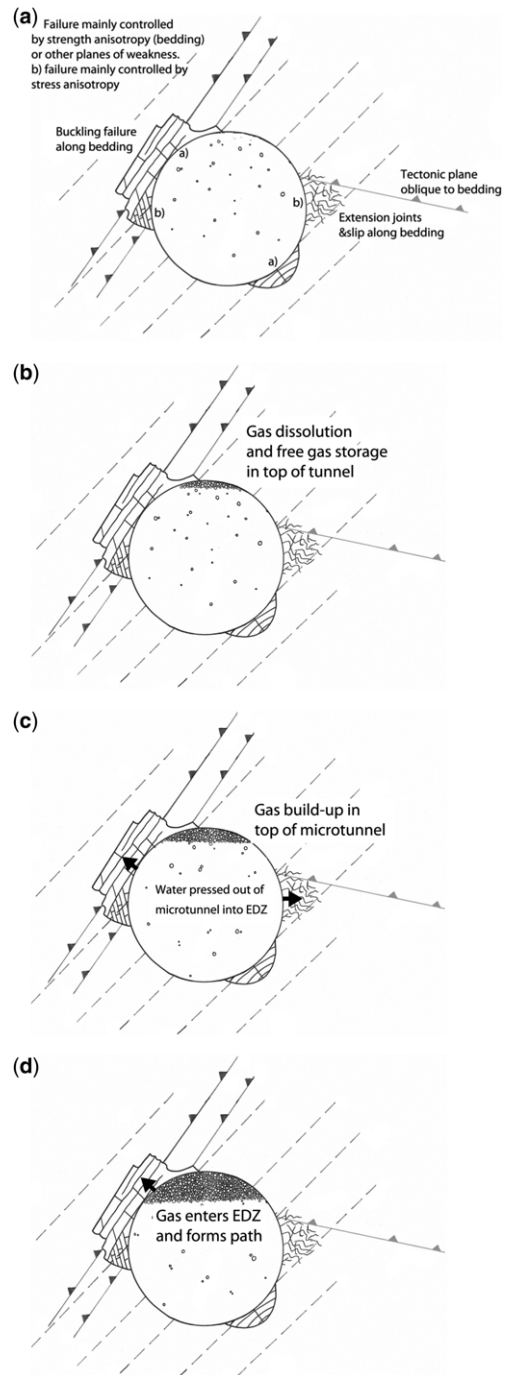


Fig. 10. EDZ schematic (from Marschall *et al.* 2008) with stages of gas injection: (a) EDZ structure; (b) storage and dissolution with linear pressure response (c. 20 days); (c) storage and leakage, pressure flattens prior to breakdown; and (d) breakdown and gas flow into the EDZ. View looking towards end of microtunnel.

SELF-SEALING AND GAS INJECTION TESTS

better match than the uniformly permeable model, but that it is not possible to discriminate between the two EDZ models (2 and 3), both with an effective EDZ conductance of $3 \times 10^{-10} \text{ m}^3 \text{ s}^{-1}$. This slightly higher value of conductance, compared with that from the sealing index, may reflect the inclusion of the resistance to flow out of the test section and to the constant head boundary imposed at the liner.

Within the models the permeability of the cylindrical EDZ (model B) is 1–2 orders of magnitude greater than the undisturbed host rock, while that of a narrow channel would be higher but of smaller cross-section area.

Discussion

Test section behaviour

The observed response of the test section to gas injection suggests that the dominant pre-breakdown processes are: test section compressibility, gas dilution in pore-water and water leakage from the test section. These result in (a) an initial storage period with linear log–log response, followed by (b) a transitional period when leakage becomes important as test section pressure rises and (c) a final breakdown when the gas level in the micro-tunnel has been driven down to the point where the gas column is in contact with a permeable feature and gas overpressure is sufficient to enter the feature, as illustrated in Figure 10.

Independent of the gas injection rate, the peak pressures during gas injection are in the order of 1.3–1.4 MPa, suggesting that gas breakthrough is controlled by the percolation process in the sparse channel network along the EDZ. No evidence of gas-‘fracturing’ was observed. Test section pressures at peak (c. 1350 kPa) and during continuing gas injection (c. 1025 kPa) were well below the measured radial stress along the seal section (minimum of eight sensors, 1950 kPa) and no unusual responses to the breakdown were observed in the seal section.

Gas flow in the EDZ

The pressure data support a model of a heterogeneous EDZ/contact zone along the sealing section with a potential channel associated with the 3 o’clock position (close to one of the notches observed immediately after excavation). However, this channel appears to be poorly connected to any outflow from the system (atmospheric boundary condition). The 6 o’clock sensor at 8.6 m shows high pressures after degassing, suggesting that it is not well connected to the test section. The small oscillations and build-ups also observed suggest

either a meta-stable or developing gas flow field rather than steady flow through an established pathway. The analysis of the pore pressure measurements in response to the gas injections gives clear evidence for localized gas leak-off along the EDZ.

Self-sealing and post-gas hydraulics

The water injections following the gas injection sequence confirmed a long-term sealing tendency of the EDZ. The effective conductance showed an ongoing reduction during saturation and hydraulic testing. Following gas injection the effective conductance swiftly reduced to values comparable to those prior to gas injection. The test zone response suggests a relatively linear flow (e.g. in a channel or some part of a cylindrical shell with conductance $c. > 5 \times 10^{-10} \text{ m}^3 \text{ s}^{-1}$).

This work was supported by ANDRA, BGR, Nagra and NWMO via the Mont Terri Consortium. The authors would like to thank the management and staff of the consortium together with the many contractors who have supported the experiment for their invaluable assistance in the technical planning and performance of the experiment.

References

- BLÜMLING, P., BERNIER, F., LEBON, P. & MARTIN, C. D. 2007. The excavation damaged zone in clay formations time-dependent behaviour and influence on performance assessment. *Chemistry of the Earth*, **32**, 588–599.
- BOCK, H. 2000. *RA Experiment – Rock Mechanics Analyses and Synthesis: Data Report on Rock Mechanics*. Mont Terri Technical Report TR 2000-02.
- BOCK, H., DEHANDSCHUTTER, B., MARTIN, C. D., MAZUREK, M., DE HALLER, A., SKOCZYLAŚ, F. & DAVY, C. 2010. *Self-sealing of Fractures in Argillaceous Formations in the Context of Geological Disposal of Radioactive Waste Review and Synthesis Report*. OECD NEA 6184. Waste Management. NEA, OECD, Paris.
- BOSSART, P., MEIER, P. M., MOERI, A., TRICK, T. & MAYOR, J.-C. 2004. Structural and hydrogeological characterisation of the excavation-disturbed zone in the Opalinus Clay (Mont Terri Project, Switzerland). *Applied Clay Science*, **26** (Clays in Natural and Engineered Barriers for Radioactive Waste Confinement), 429–448.
- CORKUM, A. G. & MARTIN, C. D. 2007. Modelling a mine-by test at the Mont Terri rock laboratory, Switzerland. *International Journal of Rock Mechanics and Mining Sciences*, **44**, 846–859, <http://dx.doi.org/10.1016/j.ijrmms.2006.12.003>
- FORGE. 2009. Fate of Repository Gases. Collaborative Project of the European Commission, part of the 7th EURATOM framework (2009–2013), <http://www.bgs.ac.uk/forge/>
- LANYON, G. W., MARSCHALL, P., TRICK, T., DE LA VAISSIÈRE, R., SHAO, H. & LEUNG, H. 2009.

- Hydromechanical evolution and self-sealing of damage zones around a microtunnel in a claystone formation of the Swiss Jura Mountains. In: *43rd U.S. Rock Mechanics Symposium & 4th U.S. – Canada Rock Mechanics Symposium*, 28 June to 1 July 2009, Asheville, NC, 652–663, paper 09-333.
- MARSCHALL, P., CROISÉ, J., SCHLICKENRIEDER, L., BOISSON, J.-Y., VOGEL, P. & YAMAMOTO, S. 2004. Synthesis of hydrogeological investigations at the Mont Terri site (phases 1 to 5). In: HEITZMANN, P. (ed.) *Mont Terri Project- Hydrogeological Synthesis, Osmotic Flow*. Reports of the Federal Office for Water and Geology, FOWG, Geology Series No. 6, Federal Office for Water and Geology, FOWG, Bern.
- MARSCHALL, P., DISTINGUIN, M., SHAO, H., BOSSART, P., ENACHESCU, C. & TRICK, T. 2006. Creation and evolution of damage zones around a microtunnel in a claystone formation of the Swiss Jura Mountains. In: *SPE International Symposium and Exhibition on Formation Damage Control*, SPE Paper 98537, Society of Petroleum Engineers, Richardson, Texas.
- MARSCHALL, P., TRICK, T., LANYON, G. W., DELAY, J. & SHAO, H. 2008. *Hydro-mechanical Evolution of Damaged Zones around a Microtunnel in a Claystone Formation of the Swiss Jura Mountains*. ARMA, San Francisco, CA.
- MARTIN, C. & LANYON, G. 2003. Measurement of in-situ stress in weak rocks at Mont Terri Rock Laboratory, Switzerland. *International Journal of Rock Mechanics and Mining Sciences*, **40**, 1077–1088, [http://dx.doi.org/10.1016/S1365-1609\(03\)00113-8](http://dx.doi.org/10.1016/S1365-1609(03)00113-8)
- MARTIN, C. D., LANYON, G. W., BLÜMLING, P. & MAYOR, J.-C. 2002. The excavation disturbed zone around a test tunnel in the ppalinus clay. In: *Proceedings of 5th North American Rock Mechanics Symposium and 17th Tunnelling Association of Canada Conference: NARMS/TAC 2002*, University of Toronto Press, Toronto, **2**, 1581–1588.
- NAGRA. 2002. *Projekt Opalinuston – Synthese der wissenschaftlichen Untersuchungsergebnisse. Entsorgungsnachweis für abgebrannte Brennelemente, verglaste hochaktive sowie langlebige mittelaktive Abfälle*. Nagra Technical Report **NTB 02-03**. Nagra, Wettingen, Switzerland.
- PEARSON, F. J., ARCOS, D. *ET AL.* 2003. *Geochemistry of Water in the Opalinus Clay Formation at the Mont Terri Laboratory*. Report of the Federal Office for Water and Geology (Bern, Switzerland), Geology Series, **5**.
- THURY, M. & BOSSART, P. 1999. The Mont Terri Rock Laboratory, a new international research project in a mesozoic shale formation, in Switzerland. *Engineering Geology*, **52**, 347–359.